Journal of Solid State Chemistry 183 (2010) 27–32

Contents lists available at ScienceDirect

Journal of Solid State Chemistry

journal homepage: www.elsevier.com/locate/jssc

Chemical and electronic characterization of cobalt in a lanthanum perovskite. Effects of strontium substitution

Jose L. Hueso [1], Juan P. Holgado, Rosa Pereñíguez, Simon Mun [2], Miquel Salmeron [2], Alfonso Caballero *

Instituto de Ciencia de Materiales de Sevilla (CSIC—University of Seville) and Departamento de Química Inorganica, Universidad de Sevilla, Avda. Américo Vespucio 49, 41092 Seville, Spain

ARTICLE INFO

Article history:
Received 26 June 2009
Received in revised form
7 October 2009
Accepted 15 October 2009
Available online 22 October 2009

Keywords:
Cobaltites
Perovskites
XAS
EXAFS
XANES
NEXAFS
Crystal field splitting

ABSTRACT

Two different cobaltites, $LaCoO_3$ and $La_{0.5}Sr_{0.5}CoO_{3-\delta}$, have been prepared and characterized by means of high energy Co K-edge and low energy O K-edge X-ray absorption spectroscopy (XAS). Even though half of the La(III) is substituted by Sr(II), little or no changes can be detected in the formal oxidation state of cobalt atoms. The presence of strontium cations induces two main effects in the chemical and electronic state of the perovskite. The charge balance with Sr(II) species is reached by the formation of oxygen vacancies throughout the network, which explains the well-known increase in the reactivity of this substituted perovskite. O K-edge XAS experiments show that the Sr(II) species induce the transitions of *d* electrons of cobalt cations from low to high spin configuration. We propose that this change in spin multiplicity is induced by two cooperative effects: the oxygen vacancies, creating five coordinated cobalt atoms, and the bigger size of Sr(II) cations, aligning the Co–O–Co atoms, and favoring the overlapping of π-symmetry cobalt and oxygen orbitals, reducing the splitting energy of e_g and t_{2g} levels.

1. Introduction

Oxides with perovskite structure (ABO_3), where A and B are metallic cations of different sizes, are of scientific interest because of their relevant electric, magnetic or catalytic properties [1–6]. Many papers have been published in recent years related with the partial substitution of atoms A and/or B, which allows for a controlled modification of most of these properties. Strontium-substituted lanthanum cobalt and others oxides with perovskites structure ($La_{1-x}Sr_xCoO_{3-\delta}$) have been extensively investigated in last years because of their relevant magnetic properties (some of them exhibiting giant magnetoresistance at low temperatures [7]), or its use as cathode material in high temperature fuel cells [8,9]. They are also interesting for their catalytic properties in the oxidation of hydrocarbon and soots, and the decomposition of nitrogen oxides [10]. Moreover, some authors have found that the low spin configuration of the $LaCoO_3$ perovskite at room temperature changes to a higher spin configuration by increasing the temperature or introducing Sr(II) atoms, also associated with changes in magnetic and conducting properties [11–15]. In spite of that, there is no general agreement about the origin of these relevant characteristics. So, while some authors suggest that these new properties are induced by Co(IV) ions stabilized in the Strontium-substituted perovskites, others attribute them exclusively to the generation of oxygen vacancies compensating the divalent charge of Sr atoms [9,16,17].

The aim of our research has been to clarify the chemical and electronic modifications of this Strontium-substituted perovskites by means of X-ray absorption spectroscopies. Combining high energy Co K-edge (extended X-ray absorption spectroscopy, EXAFS, and X-ray absorption near-edge structure, XANES) and low energy O K-edge X-ray absorption spectroscopy (XAS), light has been shed about the oxidation states and the spin configurations of $LaCoO_3$ and $La_{0.5}Sr_{0.5}CoO_{3-\delta}$ perovskites.

2. Experimental

2.1. Preparation method

The perovskite catalysts, $La_{0.5}Sr_{0.5}CoO_{3-\delta}$ and $LaCoO_3$, were synthesized by spray pyrolysis according to the methodology describes elsewhere [18,19]. The preparation method involves the uniform nebulization of nitrate solutions containing $La(NO_3)_3 \cdot 6H_2O$ (99.99%, Aldrich), $Co(NO_3)_2 \cdot 6H_2O$ (> 98%, Fluka), and $Sr(NO_3)_2$ (> 99%, Fluka), prepared as a 0.1 M liquid solution of precursors. Two online furnaces, at 250 and 600 °C, evaporate the

* Corresponding author.
E-mail address: caballero@us.es (A. Caballero).
[1] Present address. Department of Chemical Engineering, The University of Texas at Austin, Austin, TX 78712-1062, USA.
[2] Molecular Foundry, Lawrence Berkeley National Laboratory, Berkeley, CA 94720, USA.

0022-4596/$ - see front matter © 2009 Elsevier Inc. All rights reserved.
doi:10.1016/j.jssc.2009.10.008

solvent (distilled water) with the dissolved nitrates and produce an initially amorphous perovskite powder. The material was collected by a porous quartz frit located at the outlet of the heating system. Then the amorphous powders were annealed at 600 °C for 4 h, thus obtaining $LaCoO_3$ and $La_{0.5}Sr_{0.5}CoO_{3-\delta}$ crystalline perovskites with rhombohedral symmetry [18].

2.2. Characterization techniques

XRD analysis of the samples before and after treatment was performed in a Siemens D-500 diffractometer working in a Bragg–Bentano configuration, using a Cu anode under an applied voltage of 36 kV and current of 26 mA. XRD spectra were recorded with a step size of 0.02° and an accumulation time of 10 s per step.

High energy X-ray absorption spectra (XAS) were recorded at the BM25 beam line (SPLINE) of the ESRF synchrotron (Grenoble, France). XAS spectra (EXAFS and XANES regions) were acquired at room temperature in transmission mode, using self-supported wafers of the perovskite samples. In all cases the pellets were prepared using the optimum weight to maximize the signal-to-noise ratio in the ionization chambers ($\log I0/I1 \approx 1$). For energy calibration, a standard Co foil was introduced after the second ionization chamber ($I1$) and measured simultaneously. Typical XAS spectra of Co K-edge were recorded from 7500 to 8700 eV, with a variable step energy value, with a minimum 0.5 eV step across the XANES region. Once extracted from the XAS spectra, the EXAFS oscillations were Fourier transformed in the range 2.0–12.0 $Å^{-1}$. In some cases, spectra were analyzed/simulated using the software package IFEFFIT [20]. The theoretical paths for Co–Co and Co–O species used for the fitting of the experimental data were generated using the FEFF 7.0 program [21]. The coordination numbers, interatomic distance, Debye–Waller factor, and inner potential correction were used as variable parameters for the fitting procedures. Because of the high complexity of the perovskite structure (eight different coordination shells below 4.5 Å) no fitting procedure has been accomplished in most cases. However, a direct comparison of position and intensity of main peaks in the FT allows figuring out the significant structural information contained on it. Reference spectra for CoO, Co_3O_4, and metallic Co were recorded using standard reference samples.

Low energy X-ray absorption spectra (XAS) at the O K-edge were collected at the beamline 9.3.2 of the advanced light source (ALS) at Lawrence Berkeley National Laboratory using total electron yield as detection method. The energy resolution was about 3000 $E/\Delta E$ at the oxygen K edge. The base pressure of the chamber during the experiments was better than 10^{-8} Torr. The powder samples were pressed and the wafers were evacuated in situ at 200 °C for eliminating the surface contaminants.

3. Results and discussion

3.1. Structural and chemical characterization of cobaltites

After the spray pyrolysis preparation, the $LaCoO_3$ and $La_{0.5}Sr_{0.5}CoO_{3-\delta}$ solids were amorphous. However, after calcination at 600 °C the XRD patterns were in both cases characteristic of pure and well crystallized rhombohedrical structures (R-3c) with no presence of other minority phases [18].

The XANES spectra of these two samples before and after calcination are displayed in Fig. 1. The spectra of Co_3O_4 and CoO are also shown as references. Before calcination, both samples show an oscillation pattern after the main peak ($E > 7730$ eV) similar to that of cobalt spinel reference, indicating that these amorphous samples have the same short-range structure as this

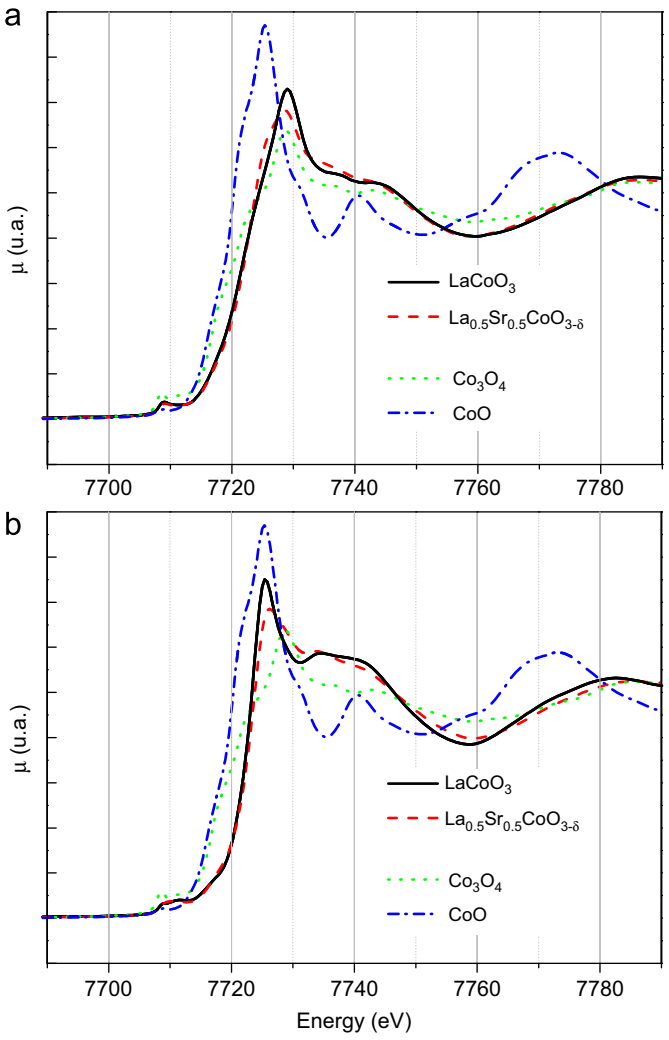

Fig. 1. Co K-edge XANES spectra of lanthanum cobaltites (a) before and (b) after calcination at 600 °C.

cobalt oxide. This conclusion agrees with the magnitude of the F.T. peaks obtained from the EXAFS spectra (Fig. 2a) where the two cobaltites and the cobalt spinel present three main peaks centered at the same distances (around 1.5, 2.5 and 3.0 Å). The third peak is much less intense for the two cobaltites, in agreement with the partially amorphous state detected by XRD. A FEFF simulation of the cobalt spinel structure [22] is included in Fig. 3. This calculation shows that the three main peaks appearing in the radial distribution function of the amorphous cobaltites can be reproduced with just four coordination shells around the tetrahedral and octahedral cobalt atoms in the spinel structure. That means that spinel-type ordered domains of around 7 Å are present in these amorphous cobaltites. Remarkably, the edge of the two samples (Fig. 1a) are shifted to higher energy than the cobalt spinel, indicating that the mean oxidation state of cobalt is higher in the cobaltites, and closer to Co(III) species.

After calcination, the XANES spectra of the cobaltites evolve to those presented in Fig. 1b, which are similar to those obtained previously by others authors for perovskite structures [7,16]. The oscillations after the edge are now clearly different from the two cobalt oxide references, and the energy of the edges, both at virtually the same position, are further shifted to higher energy. As in the $LaCoO_3$ sample the oxidation state of cobalt can be unambiguously assigned to Co(III) species, this energy value must

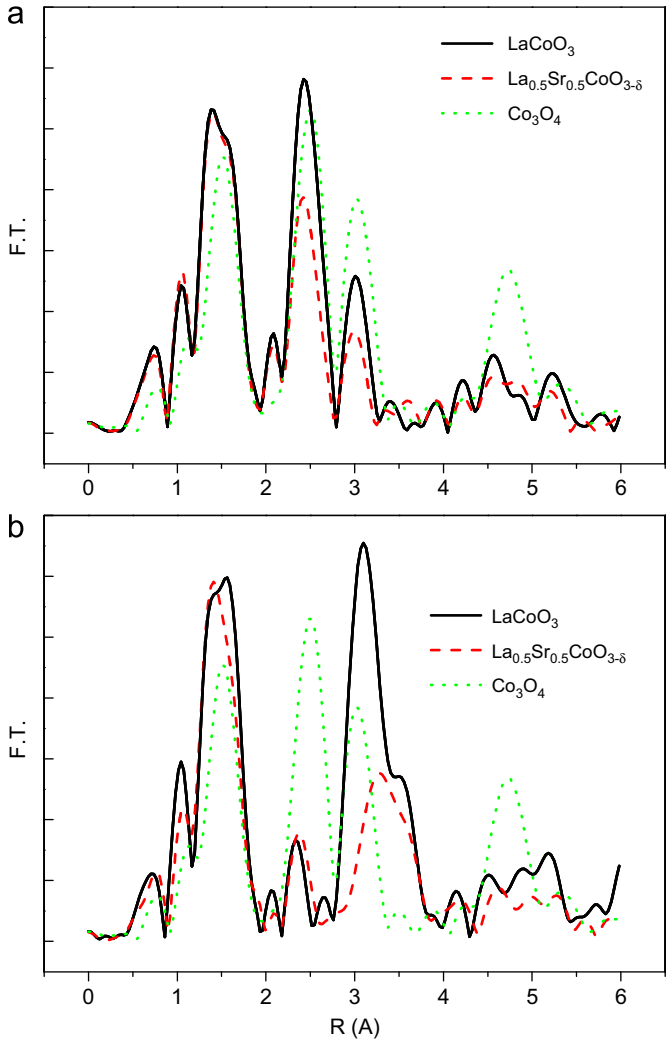

Fig. 2. F.T. of the Co K-edge EXAFS spectra of lanthanum cobaltites (a) before and (b) after calcination at 600 °C.

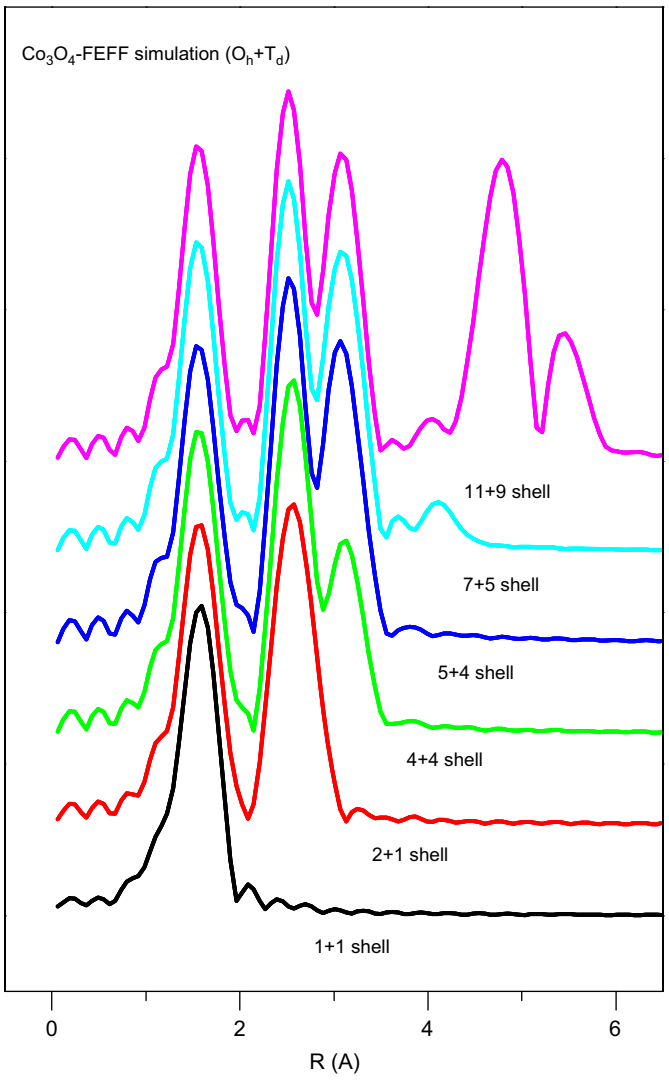

Fig. 3. FEFF simulation of the atomic environment around octahedral (O_h) and tetrahedral (T_d) cobalt atoms of Co_3O_4. The numbers at each curve refer to the number of coordination shells in the clusters for tetrahedral Co(II) and octahedral Co(III) ions.

correspond to trivalent cobalt species and so, contrary to the proposal of others authors [23], no evidence for the stabilization of Co(IV) states can be found in this XANES spectrum in our strontium substituted cobaltite. As a result, the differences in the cationic charges of La(III) and Sr(II) should be mainly compensated by oxygen vacancies in the perovskite framework, which would imply a maximum value of 0.25 for the δ stoichiometric factor of $La_{0.5}Sr_{0.5}CoO_{3-\delta}$, meaning that one out of every 12 oxygen sites are now vacant. These changes in XANES spectra come with major modifications in the F.T. magnitude of the EXAFS spectra (Fig. 2b), resulting in radial distribution functions similar to those reported previously for perovskite structures [9]. The overlapping peaks in the 3–4 Å range are much less intense for the Sr-substitute cobaltite, compatible with a sort of structural disorder caused by the oxygen vacancies present in this compound. Also, it cannot be discarded that the simultaneous presence of Sr and La in the second coordination shell of cobalt induces interferences leading to the less intense peak observed in the F.T. magnitude function.

3.2. *Crystal field effects upon Sr-substitution*

Scheme 1 shows a simplified molecular orbital diagram corresponding to cobalt coordinated by oxygen in an octahedral environment, as that of the perovskite structure. As can be seen, the overlap between O 2*p* levels and Co 3*d* orbitals splits them in t_{2g} and e_g levels. It is known that, depending on the overlap the electronic structure of d^6 Co(III) species could correspond to a low spin ($t_{2g}^6e_g^0$) or to a higher spin states ($t_{2g}^5e_g^1$ or $t_{2g}^4e_g^2$), although Co(III) compounds in a octahedral environment of oxygen have normally low spin configurations. From this scheme it is obvious that, as has been proposed previously [9], the O K-edge XAS spectra can be used to evaluate the nature of the crystal field splitting in this kind of compounds.

Fig. 4 shows the O K-edge XAS spectra of our two cobaltites, $LaCoO_3$ and $La_{0.5}Sr_{0.5}CoO_{3-\delta}$. According to the literature [9,11,24] the features in the energy range of 526–533 eV are mainly produced by transitions of the O 1*s* electrons to the Co 3*d* levels of cobalt, which are extensively mixed with the O 2*p* states. As depicted in the figure, at higher energy the La 5*d*, Co 4*s*, and 4*p* levels are also involved in the O K-edge spectra. As shown in Fig. 4 (right), the 526–533 eV region of the $LaCoO_3$ XAS is dominated by a main peak centered at around 529.6 eV, while in the Sr-substituted XAS arises a new peak at 527.6 eV. As stated before by other authors [7,11,12], this new feature, separated 2.1 eV from the first one, appears because the Sr atoms introduced

in the network induces the change from a low spin state of the Co 3*d* electrons in the $LaCoO_3$, to a high spin configuration. Now a new electronic transition to the partially empty t_{2g} levels is allowed. This change in the spin multiplicity has been explained previously considering that the presence of Sr(II) species induces the oxidation of cobalt to Co(IV), resulting in a $t_{2g}^5e_g^1$ or a $t_{2g}^4e_g^2$ electronic configuration, even though it is well known that, according to the ligand field theory [25], higher oxidation states favor low spin configurations in the split *d* orbitals.

As stated before, our XAS study allows us to suggest that the formal oxidation state of cobalt is mainly Co(III) in our two perovskites. So, changes in total positive charge produced by introducing Sr(II) species must be compensated just or mainly by oxygen vacancies in the perovskite framework.

From a chemical point of view, the observed change in the spin state of the cobalt in the perovskite induced by strontium could be explained considering two different but cooperative effects. Firstly, as a result of the oxygen vacancies formation ($La_{0.5}Sr_{0.5}CoO_{3-0.25}$), half of the cobalt ions are now five-coordinated. These cobalt cations must have a smaller crystal field splitting, reducing the concentration of high spin Co(III) species. But even the remaining six-coordinated cobalt ions are affected by structural changes induced by the Sr(II) ions. As depicted in Scheme 2, the higher ionic radius of Sr(II), 1.58 vs. 1.50 Å for La(III) [26] can lessen the rhombohedrical distortion of the perovskite structure. In fact, the structural data included also in the scheme, obtained from XRD (10) show a higher Co–Co distance in the Sr-substituted perovskite, compatible with a small expansion of the cell. This distance is closer to twice the Co–O distance in the [CoO_6] octahedron, showing that, as recognized recently by other authors [13], the Co–O–Co bond angle has increased, approaching the ideal 180° in cubic structures. As a result, almost no distortion occurs in the rhombohedrical structure of the $La_{0.5}Sr_{0.5}CoO_{3-\delta}$ substituted perovskite. Considering that the Co–O distances remain unchanged by Sr-substitution, no modification of Co–O σ-interaction must be expected. However, a better alignment of Co–O–Co atoms in two adjacent octahedrons will favor mainly the overlapping of the cobalt and oxygen orbitals with π symmetry. It is well known in chemistry that, according to the ligand field theory, this is an important factor determining the crystal field splitting of *d* levels with a π-donor ligand like $O^{=}$ species in oxides [25]. As a consequence, the presence of Sr(II) will induce a decrease in the crystal field (Scheme 3) favoring the high spin electronic configuration observed in the O K-edge XAS spectra.

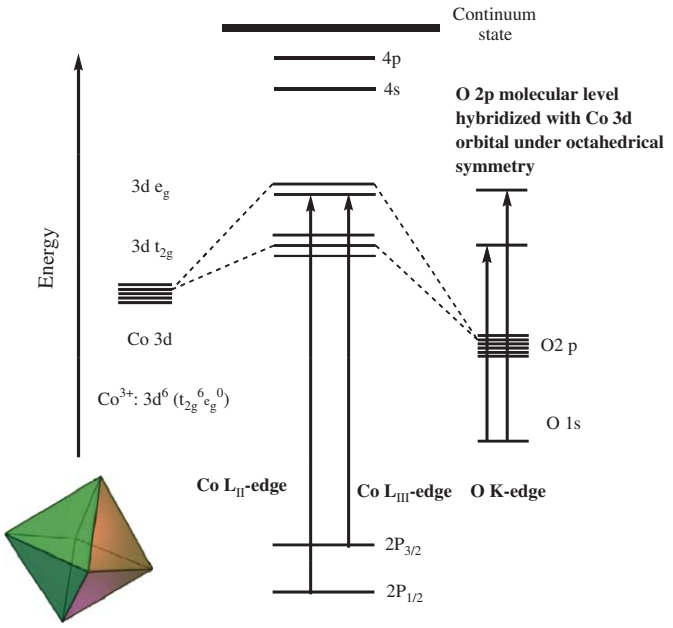

Scheme 1. Simplified molecular orbital diagram of Co(III) ions in a octahedral environment.

4. Conclusions

In summary, we have presented an XAS study of $LaCoO_3$ and $La_{0.5}Sr_{0.5}CoO_{3-\delta}$ perovskites at the Co K-edge and O K-edge. This study has shown that partial substitution of La(III) cations by Sr(II)

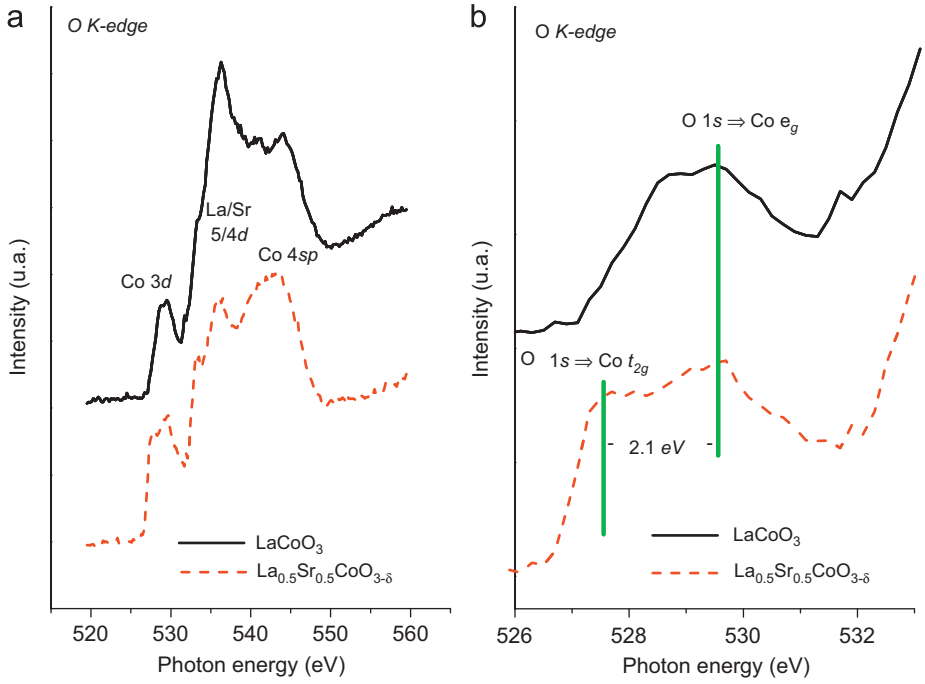

Fig. 4. (a) O K-edge X-ray absorption spectra of lanthanum cobaltites. (b) Co 3*d* bands region of the O K-edge X-ray absorption spectra.

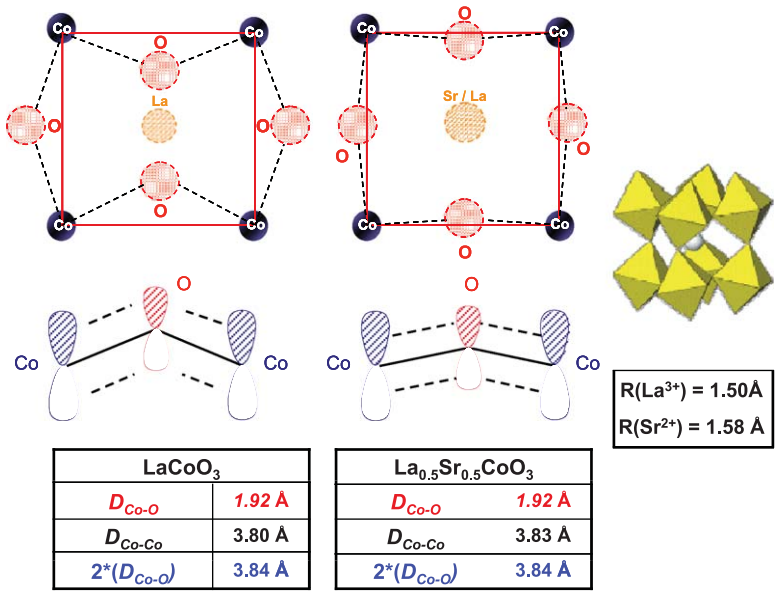

Scheme 2. Substitution of La(III) ions by the larger Sr(II) ions induces changes in the cubic environment of A atoms of ABO_3 perovskites. The geometry changes modify the orientation and overlapping of Co and O π-symmetry type orbitals.

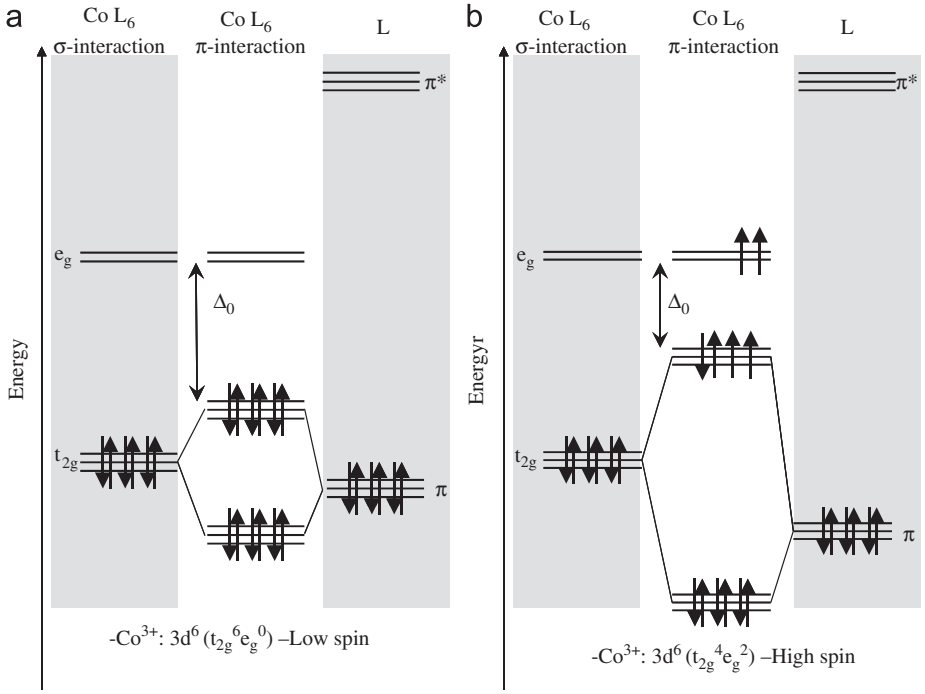

Scheme 3. Simplified molecular orbital diagram of Co(III) ions in a octahedral environment. Interaction with electronegative π-donor ligands reduces the *d* orbital splitting (left). The higher the π-interaction, the lower the orbital splitting (right), which favors high spin electronic configurations.

divalent species produces important changes in the electronic configuration of the perovskite, while no changes can be measured in the oxidation state of cobalt atoms. The generation of oxygen vacancies explains the higher reactivity of the substituted perovskite.

The results from O K-edge XAS indicate that the spin state of cobalt 3*d* electrons in the Sr-substituted perovskite changes from an initial high field, low spin state to a low field, high spin configuration. The results obtained from the Co K-edge XAS indicate that little or no changes are produced in the formal oxidation state of cobalt, which remains as a trivalent specie in the Sr-containing perovskite. All these results lead us to propose that changes in spin configuration of Co(III) in our samples can be explained considering two effects. First, the half of the cobalt ions is now five coordinated, which reduces the crystal field splitting of these metal atoms. Second, the better alignment of Co–O–Co atoms caused by the larger size of Sr(III) must contribute to modify the electronic configuration of the cobalt ions. The resulting increase in volume favors a better overlapping between cobalt and oxygen π-type orbitals, which produces an increase in

the energy of t_{2g} levels and the concomitant decrease in the ligand field splitting of Co *d* orbitals.

Acknowledgments

We thank the Ministry of Science and Education of Spain for financial support (Projects ENE2007-67926-C02-01, 2007-FQM-2520 and Mobility Action PR2007-0374ENE2004-01660). We also thank the staff of the ESRF BM25 beamline and ESRF facility (Grenoble, France) and the staff of ALS beamline 9.3.2 and ALS facility (LNBL, Berkeley, CA) for funding and helping to accomplish these experiments. MS is funded by the Office of Basic Energy Sciences, Chemical Sciences, Geosciences, and Biosciences Division, under the Department of Energy Contract no. DE-AC02-05CH11231. AC wants to thank Prof. P. Woodward for his helpful comments on the article.

References

[1] M.A. Peña, J.L.G. Fierro, Chem. Rev. 101 (2001) 1981–2017.
[2] Y. Nishihata, J. Mizuki, T. Akao, H. Tanaka, M. Uenishi, M. Kimura, T. Okamoto, N. Hamada, Nature 418 (2002) 164–167.
[3] H. Tanaka, M. Misono, Curr. Op. Solid State Mater. Sci. 5 (2001) 381–387.
[4] S. Kimura, Y. Maeda, T. Kashiwagi, H. Yamaguchi, M. Hagiwara, S. Yoshida, I. Terasaki, K. Kindo, Phys. Rev. B 78 (2008) 180403(R).
[5] J.T. Rijssenbeek, T. Saito, S. Malo, M. Azuma, M. Takano, K.R. Poeppelmeier, J. Am. Chem. Soc. 127 (2005) 675–681.
[6] S. Margadonna, G. Karotsis, J. Am. Chem. Soc. 128 (2006) 16436–16437.
[7] O. Toulemonde, N. N'Guyen, F. Studer, J. Solid State Chem. 158 (2001) 208–217.
[8] M.G. Bellino, J.G. Sacanell, D.G. Lamas, A.G. Leyva, N.E. Walse de Reca, J. Am. Chem. Soc. 129 (2007) 3066–3067.
[9] O. Haas, R.P.W.J. Struis, J.M. McBreen, J. Solid State Chem. (2004) 1000–1010.
[10] J.L. Hueso, A. Caballero, M. Ocaña, A.R. Gonzalez-Elipe, J. Catal. 257 (2008) 334–344;
N. Closset, R.v. Doorn, H. Kruidhof, J. Boeijsma, Powder Diffr. 11 (1996) 31.
[11] M. Abbate, J.C. Fuggle, A. Fujimori, L.H. Tjeng, C.T. Chen, R. Potze, G.A. Sawatzky, H. Eisaki, S. Uchida, Phys. Rev. B 47 (1993) 16124–16130.
[12] A.R. Moodenbaugh, B. Nielsen, S. Sambasivan, D.A. Fisher, T. Friessnegg, S. Aggarwal, R. Ramesh, R.L. Pfeffer, Phys. Rev. B 61 (2000) 5666.
[13] E. Efimova, V. Efimov, D. Karpinsky, A. Kuzmin, J. Purans, V. Sikolenko, S. Tiutiunnikov, I. Troyanchuk, E. Welter, D. Zajac, V. Simkin, A. Sazonov, J. Phys. Chem. Solids 69 (2008) 2187–2190.
[14] C. Pinta, D. Fuchs, M. Merz, M. Wissinger, E. Arac, H.v. Löhneysen, A. Samartsev, Phys. Rev. B 78 (2008) 174402.
[15] M.W. Haverkort, Z. Hu, J.C. Cezar, T. Burnus, H. Hartmann, M. Reuther, C. Zobel, T. Lorenz, A. Tanaka, N.B. Brookes, H.H. Hsieh, H.-J. Lin, C.T. Chen, L.H. Tjeng, Phys. Rev. Lett. 97 (2006) 176405.
[16] T. Hanashima, S. Azuhata, K. Yamawaki, N. Shimizu, T. Mori, M. Tanaka, S. Sasaki, Jpn. J. Appl. Phys. 43 (2004) 4171–4178.
[17] J.E. Sunstrom IV, K.V. Ramanujachary, M. Greenblatt, M. Croft, J. Solid State Chem. 139 (1998) 388–397.
[18] J.L. Hueso, J. Cotrino, A. Caballero, J.P. Espinos, A.R. Gonzalez-Elipe, J. Catal. 247 (2007) 288–297.
[19] E. Lopez-Navarrete, A. Caballero, V.M. Orera, F.J. Lazaro, M. Ocaña, Acta Mater. 51 (2003) 2371–2381.
[20] M. Newville, J. Synchr. Radiat. 8 (2001) 322–324.
[21] A.L. Ankudinov, J. Rehr, J. Phys. Rev. B 56 (1997) 1712.
[22] J.P. Holgado, A. Caballero, J.P. Espinos, J. Morales, V.M. Jimenez, A. Justo, Thin Solid Films 377 (2000) 460–466.
[23] F.J. Berry, J.F. Marco, X. Ren, J. Solid State Chem. 178 (2005) 961–969.
[24] M. Abbate, F.M.F. de Groot, J.C. Fuggle, A. Fujimori, O. Strebel, F. Lopez, M. Domke, G. Kaindl, G.A. Sawatzky, M. Takano, Y. Takeda, H. Eisaki, S. Uchida, Phys. Rev. B 46 (1992) 4511.
[25] C.J. Ballhausen, Introduction to Ligand Field Theory, McGraw-Hill, New York, 1962;
B.N. Figgis, M.A. Hitchman, Ligand Field Theory and Its Applications, Wiley, 2000.
[26] R.D. Shannon, Acta Crystallogr. A 32 (1976) 751–767.